NEOPLASIA
www.neoplasia.com

Volume 18 Number 8 August 2016 pp. 489–499 489

Identification and Validation of *PCAT14* as Prognostic Biomarker in Prostate Cancer[1]

Sudhanshu Shukla[*,‡,2], Xiang Zhang[*,†,2], Yashar S. Niknafs[*,2], Lanbo Xiao[*,‡,2], Rohit Mehra[*,‡], Marcin Cieślik[*,‡], Ashley Ross[§], Edward Schaeffer[§], Bhavna Malik[¶], Shuling Guo[#], Susan M. Freier[#], Huynh-Hoa Bui[#], Javed Siddiqui[*,‡], Xiaojun Jing[*,‡], Xuhong Cao[*,‡], Saravana M. Dhanasekaran[*,‡], Felix Y. Feng[*,¶,3], Arul M. Chinnaiyan[*,‡,,††,‡‡,3] and Rohit Malik[*,‡,3]**

*Michigan Center for Translational Pathology, University of Michigan, Ann Arbor, USA; [†]Department of Urology, Qilu Hospital of Shandong University, Jinan, China; [‡]Department of Pathology, University of Michigan, Ann Arbor, USA; [§]James Buchanan Brady Urological Institute, Johns Hopkins University, USA; [¶]Department of Radiation Oncology, University of Michigan, Ann Arbor, USA; [#]Ionis Pharmaceutical, CA; [**]Howard Hughes Medical Institute, University of Michigan, Ann Arbor, USA; [††]Department of Urology, University of Michigan Medical School, Ann Arbor, MI, USA; [‡‡]Comprehensive Cancer Center, University of Michigan, Ann Arbor, USA

Abstract

Rapid advances in the discovery of long noncoding RNAs (lncRNAs) have identified lineage- and cancer-specific biomarkers that may be relevant in the clinical management of prostate cancer (PCa). Here we assembled and analyzed a large RNA-seq dataset, from 585 patient samples, including benign prostate tissue and both localized and metastatic PCa to discover and validate differentially expressed genes associated with disease aggressiveness. We performed Sample Set Enrichment Analysis (SSEA) and identified genes associated with low versus high Gleason score in the RNA-seq database. Comparing Gleason 6 versus 9+ PCa samples, we identified 99 differentially expressed genes with variable association to Gleason grade as well as robust expression in prostate cancer. The top-ranked novel lncRNA *PCAT14,* exhibits both cancer and lineage specificity. On multivariate analysis, low *PCAT14* expression independently predicts for BPFS ($P = .00126$), PSS ($P = .0385$), and MFS ($P = .000609$), with trends for OS as well ($P = .056$). An RNA in-situ hybridization (ISH) assay for *PCAT14* distinguished benign vs malignant cases, as well as high vs low Gleason disease. *PCAT14* is transcriptionally regulated by AR, and endogenous *PCAT14* overexpression suppresses cell invasion. Thus, Using RNA-sequencing data we identify *PCAT14,* a novel prostate cancer and lineage-specific lncRNA. *PCAT14* is highly expressed in low grade disease and loss of *PCAT14* predicts for disease aggressiveness and recurrence.

Neoplasia (2016) 18, 489–499

Address all correspondence to: Arul M. Chinnaiyan, M.D., Ph.D., Investigator, Howard Hughes Medical Institute, American Cancer Society Professor, S. P. Hicks Endowed Professor of Pathology, Professor of Pathology and Urology, Comprehensive Cancer Center, University of Michigan Medical School, 1400 E. Medical Center Dr. 5316 CCGC, Ann Arbor, MI 48109-0602.
E-mail: arul@med.umich.edu

[1]Funding/Support: This work was supported in part by the Prostate Cancer Foundation (F.Y.F, A.M.C), the National Institutes of Health Prostate SPORE (P50CA186786 to A.M.C) and the Early Detection Research Network (U01CA111275 and U01CA113913 to A.M.C). A.M.C. is supported by the Alfred A. Taubman Institute, Howard Hughes Medical Institute and the American Cancer Society. R.M is supported by a Department of Defense postdoctoral award (W81XWH-13-1-0284). R.M. and M.C. are supported by a Prostate Cancer Foundation Young Investigator award. The sponsors played no role in the design and conduct of the study.
[2]Equal Contributions.
[3]Co-senior authors.
Received 5 July 2016; Accepted 6 July 2016

1476-5586
http://dx.doi.org/10.1016/j.neo.2016.07.001

Introduction

Early detection of prostate cancer, largely facilitated by the advent of PSA screening, has also been attributed to over-diagnosis and overtreatment of this disease [1–3]. While coupling PSA screening with other biomarkers such as the long non-coding RNA (lncRNA) transcript *PCA3* or gene fusions events (such as TMPRSS2-ERG) have increased specificity of cancer diagnosis, these biomarkers have limited utility in stratifying patients in terms of prognosis [4,5]. While stratifying patients into risk groups based on clinicopathologic features is currently used to guide treatment decisions [6], it is clear that current stratification approaches need to be further refined to allow better personalization of therapy. Thus, identifying molecular biomarkers to distinguish indolent versus aggressive disease would address an unmet need in the clinical management of prostate cancer.

Advances in next-generation sequencing technologies have enabled thorough characterization of cancer transcriptomes, especially in unraveling the realm of non-coding RNAs (ncRNAs) [7,8]. In particular, lncRNAs, a class of ncRNAs, have gained increasing attention as biomarkers due to their tissue- and cancer-specific expression profile [9]. In this study, we assembled and analyzed a large RNA-seq compendium compiled from recent publications from consortiums such as The Cancer Genome Atlas (TCGA), the Prostate Cancer Foundation/Stand Up to Cancer international team, and others to identify differentially expressed genes (both protein coding and non-coding genes), that are associated with indolent versus aggressive disease [10,11]. Our results identify *PCAT14*, a prostate cancer- and lineage-specific lncRNA, as a top differentially expressed gene in this context. We characterize *PCAT14* preclinically and demonstrate that it correlates inversely in expression with disease aggressiveness and adds to conventional clinicopathologic risk factors in predicting prognosis in prostate cancer patients. Finally, we develop a novel in-situ hybiridation (ISH)-based approach for detecting *PCAT14* in clinical samples.

Material and Methods

RNA-Seq Data Set

Prostate RNA-seq cohort (n = 585) containing 52 benign prostate tissues, 501 primary prostate cancers, and 132 metastatic prostate cancers was used in this study. For nomination of Gleason associated genes, we compared low Gleason tumors (Gleason 6, n = 45) to high Gleason tumors (Gleason 9+, n = 140).

RNA-seq Data Processing

TCGA prostate Fastq files were obtained from the CGhub. Reads were aligned using STAR version 2.4.2 [12] and read abundance was calculated using FeatureCounts version 1.4.6 [13].

RNA-Seq Differential Expression Testing

Differential expression testing was performed using the Sample Set Enrichment Analysis (SSEA) tool described previously [7]. Briefly, following count data normalization, SSEA performs the weighted KS-test procedure described in GSEA [14]. The resulting enrichment score (ES) statistic describes the enrichment of the sample set among all samples being tested. To test for significance, SSEA enrichment tests are performed following random shuffling of the sample labels. These shuffled enrichment tests are used to derive a set of null enrichment scores (1000 null enrichment scores computed). The nominal p value reported is the relative rank of the observed enrichment score within the null enrichment scores. Multiple hypothesis testing is performed by comparing the enrichment score of the test to the null normalized enrichment score (NES) distributions for all transcripts in a sample set. This null NES distribution is used to compute FDR q values in the same manner used by GSEA [14]. SSEA percentile score determined by ranking the genes in each analysis by their NES score.

Tissue Expression Heatmap Generation

The "gplots" R-package was used to generate heatmaps using the *heatmap.2* function. Expression was normalized as log2 of the fold-change over the median of the normal samples for each transcript. Unsupervised hierarchical clustering was performed with the *hclust* function, using Pearson correlation as the clustering distance, using the "ward" agglomeration method.

Identification of Genes Differentially Expressed in Prostate Cancer of Varying Gleason Score

Differentially expressed Gleason associated genes were identified as any gene with an SSEA FDR< 0.01 when comparing Gleason 6 primary tumors to Gleason 9+ primary tumors. Filtering for expression levels in tissues was done by enforcing that each gene had >5FPKM expression in the top 5% of prostate tumor samples. Filtering for overexpression in cancers versus normal was done by enforcing an SSEA FDR of <0.0001 in an analysis comparing the TCGA prostate cancer vs normal tissues. Tissue specificity percentile was determined as the SSEA percentile for each gene in an SSEA analysis comparing the TCGA prostate samples to all other TCGA tumors in our multi-tissue compendium [7].

Clinical Analysis

To assess the prognostic value of *PCAT14*, microarray data was obtained from the Johns Hopkins University (JHU) (N = 355). Patients were treated with prostatectomy and subsequently received no adjuvant or salvage treatment until metastasis. Microarray processing and normalization was performed as described previously [15]. *PCAT14* expression was calculated by taking the mean expression of probe sets mapping to exons. High/low *PCAT14* was determined by splitting on the median expression level. Kaplan–Meier curves are shown and statistical inference was performed using the Log-rank test. Multivariate analysis was performed using Cox regression. Age was treated as a continuous variable. PSA was grouped into low (<10 ng/ml), intermediate (10–20 ng/ml), and high (>20 ng/ml). Surgical margin status (SMS), seminal vesicle invasion (SVI), extracapsular extension (ECE), and lymph node invasion (LNI) were treated as binary variables. Gleason score was grouped into low (≤7) or high (8–10). Association of *PCAT14* and clinicopathologic variables was evaluated using a *t*-test for continuous variables, and a chi-squared test for categorical variables. Statistical significance was set as a two-sided *p*-value <0.05. All analyses were performed in R 3.1.2.

ISH Analysis

PCAT14 ISH was performed on thin (approximately 4 μm thick) TMA sections (Advanced Cell Diagnostics, Inc., Hayward, CA), as described previously [16,17]; in parallel, *PCAT14* ISH was performed on previously identified positive and negative control index formalin-fixed paraffin embedded (FFPE) tissue sections. All slides were examined for *PCAT14* ISH signals in morphologically intact cells and scored manually by a study pathologist (Rohit Mehra). Specific *PCAT14* ISH signal was identified as brown, punctate dots, and expression level was scored as follows: 0 = no staining or less than 1 dot per 10 cells, 1 = 1 to 3 dots per cell, 2 = 4 to 9 dots per cell (few

or no dot clusters), 3 = 10 to 14 dots per cell (less than 10% in dot clusters), and 4 = greater than 15 dots per cell (more than 10% in dot clusters). For each evaluable tissue core, a cumulative ISH product score was calculated as the sum of the individual products of the expression level (0 to 4) and percentage of cells (0 to 100) (i.e., [A% × 0] + [B% × 1] + [C% × 2] + [D% × 3] + [E% × 4]; total range = 0 to 400). For each tissue sample, the ISH product score was averaged across evaluable TMA tissue cores. All quantitative data were shown as mean ± S.D. To obtain significance in the difference between two groups was performed by two-sided t test using Graph Pad Prism 6.02 software.

Cell Lines, Tissues and Reagents

All prostate cell lines used in this study were purchased from the American Type Culture Collection (ATCC), cultured according to their recommendations and were periodically checked for mycoplasma contamination and genotyped to confirm identity. For androgen treatment experiments, VCaP cells were pre-cultured in androgen-free charcoal-stripped medium for 48 hours and treated with 10 nM dihydrotestosterone (DHT) or 10 μM MDV3100 or vehicle (ethanol) for indicated time points before cells were harvested for RNA isolation. For drug treatment experiments, LNCaP cells were treated with the 5–20 μM DNA methylation inhibitor 5-aza-2′-deoxycytidine (5-aza) (catalog: A3656-5MG, Sigma), or DMSO for 5 days. RNA was isolated 24 h after drug treatment and expression was analyzed by qRT-PCR.

Prostate specimens were acquired from the patients who underwent radical prostatectomy and from the Rapid Autopsy Program at the tissue core of University of Michigan as part of the University of Michigan Prostate Cancer Specialized Program Of Research Excellence (S.P.O.R.E.). Informed consents were obtained from each patient.

RNA Isolation and qPCR Analysis

Total RNA was extracted using Trizol reagent and an RNeasy Micro Kit (Qiagen) with DNase I digestion according to the manufacturer's protocols. RT-PCR was performed from total RNA using Superscript III (Invitrogen) with random primers (Invitrogen). Quantitative PCR (qPCR) was performed using Fast SYBR Green Master Mix (Applied Biosystems) on a 7900HT Fast Real-Time PCR system (Applied Biosystems). All oligonucleotide primers were purchased from Integrated DNA Technologies (Coralville, IA) are sequence of each primer is listed in Supplementary Table 4. Primer specificity was determined by sequence verifying the PCR products using the University of Michigan Sequencing Core facility.

Rapid Amplification of cDNA Ends (RACE)

5′ and 3′ RACE was performed using the GeneRacer RLM-RACE kit (Invitrogen) according to the manufacturer's protocols. RACE PCR products obtained using Platinum Taq high-fidelity polymerase (Invitrogen), were resolved on a 1.5% agarose gel. Individual bands were gel purified using a Gel Extraction kit (Qiagen), and cloned into PCR4 TOPO vector, and sequenced using M13 primers.

Knock Down Studies

MDA-PCa-2b and VCaP cells were seeded in biocoated 6-well plates at 60% confluency, incubated overnight, and transfected with 50 nM siRNAs targeting different exons of *PCAT14* or non-targeting siRNAs, using RNAi MAX reagent (Invitrogen) per manufacturer's instructions. RNA was harvested 48 h after transfection. Functional experiments were performed at indicated time points. Sequence of all the siRNA used in shown in Supplementary Table 4.

Nuclear-Cytoplasmic Subcellular Fractionation

Nuclear-cytoplasmic fraction of MDA-PCa-2b and VCaP cells was performed using an NE-PER Nuclear and Cytoplasmic Extraction kit (Thermo Scientific) following manufacturer's instructions, followed by RNA isolation and qPCR analysis.

CRISPR Based Overexpression of PCAT14

Stable cell lines overexpressing *PCAT14* endogenously were made using previously published protocol [18]. Briefly, guide RNAs targeting promoter region of *PCAT14* (Supplementary Table 4) were designed using online tool at http://crispr.mit.edu/ and cloned into sgRNA-MS2 vector using lenti sgRNA(MS2) zeo backbone. Lentiviral particles expressing *PCAT14* sgRNA-MS2 were generated by the University of Michigan vector core. To generate LNCaP or PC3 cell over expressing *PCAT14*, first cells were seeded into 100 mm dish and transduced with Lenti dCAS-VP64 (blasticidin) and Lenti-MS2-p65-HSF1 (hygromycin) vectors. After 2 days, cells were selected with 4 μg/ml Blasticidin and 200 μg/ml Hygromycin. Cells stably expressing dCAS-VP64 and MS2-p65-HSF1 cells were then seeded in 6-well plates and infected with *PCAT14* sgRNA-MS2 lentivirus. 24 hours later, cells were selected with triple antibiotics: 4 μg/ml Blasticidin, 200 μg/ml Hygromycin and 800 μg/ml Zeomycin for 1 week. Expression of *PCAT14* in these cells was verified by qPCR.

In Vitro FluoroBlok Tumor Invasion Assay

The In vitro FluoroBlok Tumor Invasion Assay (BD) was performed as previously described [19]. Briefly, after rehydration of the BD FluoroBlok membrane, 500 ul of serum-free RPMI medium resuspended prostate cancer cells (PC3, 50,000 cells per well, or LNCaP, 100,000 cells per well) were seeded into the apical chambers. 750 ul RPMI medium containing 10% FBS were added to the basal chamber as chemoattractant. Then plates were incubated at 37 °C, 5% CO_2 for 24 hours. Following incubation, medium from the apical chambers were removed, and the inserts were transferred to a 24-well plate containing 500ul/well of 4ug/mL Calcein AM (Invitrogen) in Hanks buffered saline. Plates were incubated for 1 hour at 37 °C, 5% CO_2, then pictures of invaded cells were taken by using inverted fluorescence microscope (Olympus), and quantified by ImageJ software [20].

Oncomine Concepts Analysis of the PCAT14 Signature

Gene that positively correlated ($R^2 > 0.35$, n = 591) with *PCAT14* in TCGA RNA-seq data were selected and uploaded into Oncomine database [21] as custom concepts (Supplementary Table 2). All the prostate cancer concepts with odds ratio> 2.0 and *p*-value $<1 \times 10^{-4}$ were selected. For simplicity, top 4 concepts (based on odds ratios) were selected for representation. We exported these results as the nodes and edges of a concept association network and visualized the network using Cytoscape version 3.3.0. Node positions were computed using the Edge-weighted force directed layout in Cytoscape using the odds ratio as the edge weight. Node positions were subtly altered manually to enable better visualization of node labels.

Statistics

All quantitative data were shown as mean ± S.D. To obtain significance in the difference between two groups was performed by two-sided t test or ANOVA using Graph Pad Prism 6.02 software.

Results

Identification of Genes Associated With Gleason Grade in Prostate Cancer

Comprehensive molecular characterization of common cancer types has become feasible with the recent availability of large next generation sequencing datasets on tumor tissues. To identify genes (both coding and non-coding) associated with aggressive prostate

cancer, we assembled a large prostate RNA-seq cohort (n = 585) containing 52 benign prostate tissues, 501 primary prostate cancers, and 132 metastatic prostate cancers. We performed differential expression testing utilizing a non-parametric tool we developed for RNA-seq data called Sample Set Enrichment Analysis [7]. In order to nominate the most intriguing biomarkers associated with aggressive disease, we compared low Gleason tumors (Gleason 6, n = 45) to high Gleason tumors (Gleason 9+, n = 140) and applied filters for substantial expression in prostate tumor tissue (>5PKM in the top 5% of prostate samples), and significant differential expression in

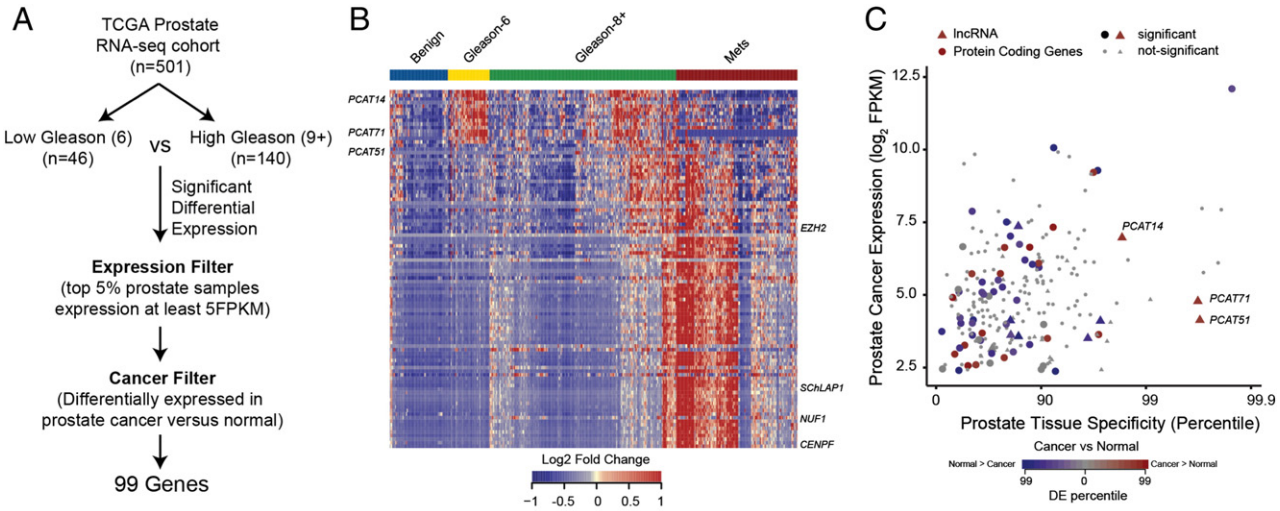

D

Gene Name	Category	Gleason 9+ Percentile	Prostate Expression (95%ile FPKM)	Cancer vs Normal Percentile	Tissue Sepcificity Percentile
PCAT14	lncRNA	99.57	125.589	97.93	98.40
TSPAN1	Protein coding	99.63	594.854	98.05	96.92
PTRHD1	Protein coding	99.38	160.925	99.03	92.41
DUS1L	Protein coding	99.57	99.683	99.02	87.25
GMDS	Protein coding	99.91	99.117	98.31	77.82

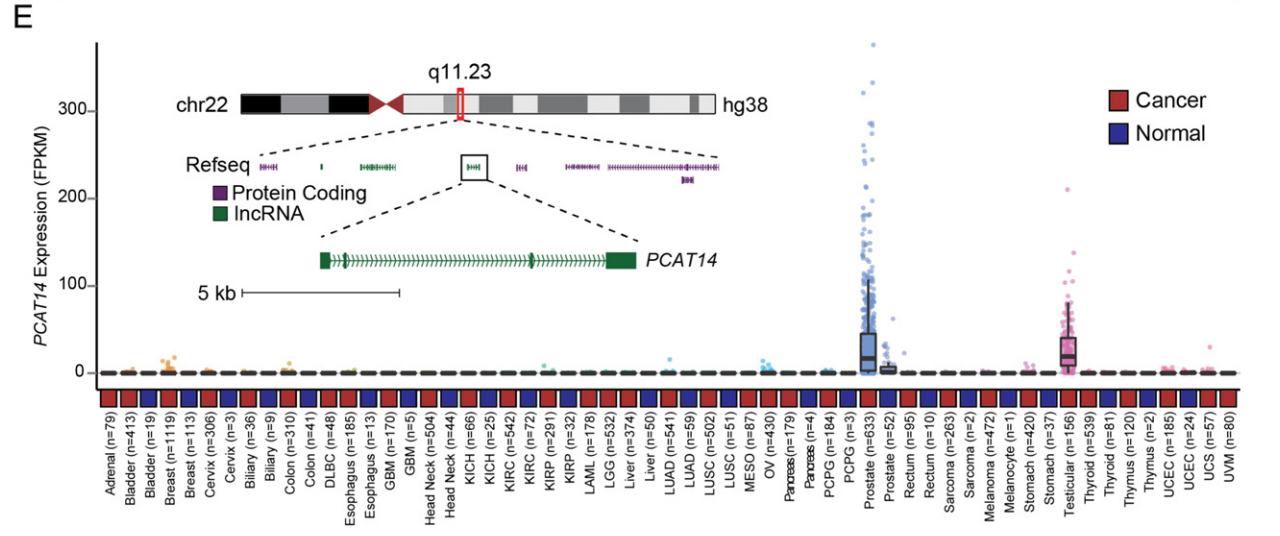

Figure 1. Identification of lncRNA *PCAT14* as a prostate cancer biomarker. A. Schematic representation of the workflow utilized to identify highly-expressed, prostate cancer specific genes associated with low-Gleason disease. B. Heatmap depiction of the lncRNA and protein coding genes differentially expressed (n = 99) between Gleason 6 versus 9+ analysis in TCGA prostate RNA-seq data. Relative expression of these genes in benign and metastatic prostate cancer tissues [11] are also displayed alongside for comparison. Expression is depicted as log2 of the fold-change over the median of the Gleason 6 samples for each gene. Patients grouped by cancer progression/Gleason score. Rows represent genes and columns represent samples. C. Scatterplot showing the expression level, prostate tissue specificity, and prostate cancer association of protein coding (solid circle) and lncRNA (solid triangles) genes identified in 1 A. Expression is represented by the FPKM value for the 95th percentile prostate cancer sample. Cancer versus normal and prostate tissue specificity are represented by the percentile score for each gene in an SSEA analysis. D. The top five, Gleason 6 associated genes listed in the order of prostate tissue specificity. E. Expression of *PCAT14* across all cancer and normal tissue type represented in the TCGA. Inset shows genome browser view of *PCAT14* genomic location.

prostate cancers versus normal (SSEA, FDR <0.0001) leaving a total of 99 candidates genes (Figure 1*A*, Supplementary Table 1). Interestingly, clustering analysis revealed signature expression patterns, specifically associated with low, high Gleason and metastatic status and included both novel and previously characterized genes (Figure 1*B*). *CENPF* and EZH2, protein coding genes with a known association with high grade prostate cancer were rediscovered through this analysis [22,23]. Similarly, we rediscovered *SChLAP1* a long non-coding RNA (lncRNA) associated with aggressive prostate cancers [15,17] in our analysis (Figure 1*B*). With the goal of identifying potential biomarkers that distinguish indolent prostate cancers, we focused on genes enriched in low grade disease that are expressed highly in prostate tissue and that also show prostate cancer and tissue specificity (Figure 1*C*). Interestingly, a lncRNA, *PCAT14* appeared to be one of the top low-Gleason-associated genes with robust prostate tissue expression, substantial prostate tissue specificity, and significant overexpression in prostate cancers versus normal (Figure 1*D*). In fact, among all genes (coding and non-coding), *PCAT14* ranked among the top 5 in terms of expression level, Gleason 6 versus 9+ association, and cancer versus normal association (Figure 1*D*). Additionally, among the top 5 candidate genes, *PCAT14* was the only gene to exhibit striking prostate tissue specificity, a particularly relevant metric for a potential biomarker (Figure 1*E*). The remaining 4 genes exhibited variable prostate tissue specificity (Supplementary Figure 1). *PCAT14* is a poly-exonic gene found within a gene desert on chromosome 22, with a striking prostate cancer and lineage specific expression pattern across the >10,000 TCGA cancer and normal tissue samples (Figure 1*E*). For these reasons, we elected to pursue *PCAT14* as a promising biomarker that can identify low grade prostate cancer.

Genomic Organization and Regulation of PCAT14

We collected multiple lines of evidence from both experimental data and available annotations to consolidate the genomic organization of *PCAT14*. Based on assembled reads from RNA-seq data assembled in the MiTranscriptome [7], we predicted the structure of the *PCAT14* transcript variants (Supplementary Figure 1A). Additionally, as an independent approach to define the exon structure of *PCAT14,* we performed rapid amplification of cDNA ends (RACE) in two prostate cancer cell lines VCaP and MDA-PCa-2b that express *PCAT14* at high levels (Supplementary Figure 1B and C). Our analyses show that the *PCAT14* gene is located on chr22-q11.2 and contains 4 exons. Among the four transcript isoforms, the 2.3 kb variant-1 demonstrates the highest expression (Supplementary Figure 1D). Next, using published ChIP-seq data in VCaP cells [24], we show that *PCAT14* has all the histone marks (H3K4me3, H3K36me3, H3K27ac) associated with actively transcribed genes (Figure 2A). We further performed subcellular fractionation followed by qPCR to show that *PCAT14* is distributed equally between nuclear and cytoplasmic compartments (Figure 2*B*).

Androgen receptor plays a major role To identify any potential regulation of *PCAT14* gene by androgen, we assessed the presence of AR peaks in *PCAT14* genomic region using AR-ChIP-seq data generated in VCaP cells [24] and saw significant AR peaks in *PCAT14* loci. Some of these peaks were also enhanced upon treatment with DHT and were suppressed upon treatment with AR antagonist MDV3100 or bicalutamide (Figure 2*C*). To corroborate this finding, we assessed the expression of *PCAT14* mRNA in VCaP cells upon AR stimulation. Similar to the canonical AR targets such as *KLK3* and *FKBP5*, *PCAT14* expression was also significantly elevated (four fold in 24 hours) upon DHT stimulation (Figure 2*D*) and suppressed by MDV3100 treatment (Figure 2*E*). In another line of investigation, we queried if epigenetic regulation might play a role in the prostate cancer and lineage specific expression of *PCAT14* observed in tissue samples (Figure 1*E*). Using a prostate cancer cell line (LNCaP) model we show significant elevation of *PCAT14* expression when treated with 5-azacytidine (5-Aza), a DNA demethylation agent, suggesting a potential role for promoter methylation in regulation of *PCAT14* (Figure 2*F*). However, our attempt to capture this event in TCGA tissue samples where Infinium 450 K DNA methylation array data is available was inconclusive, due to the lack of probes in *PCAT14* promoter region. Taken together we show *PCAT14* is an AR target gene that may also be subjected to epigenetic regulation in prostate cancer.

Clinical Association of PCAT14

Having observed an inverse correlation of *PCAT14* with Gleason Score (GS) in our RNA-seq cohort, we next assessed the association of *PCAT14* expression with clinical outcomes in prostate cancer. For this analysis we first divided samples into 7 groups (benign, GS-6, GS-7 (3 + 4), GS7 (4 + 3), GS-8, GS-9 and Mets) and examined the expression of *PCAT14* using two different datasets (TCGA and Taylor et al.). We identified a significant decrease in *PCAT14* expression as Gleason grade increased in both cohorts (Figure 3*A* and *B*). Importantly, in the large TCGA dataset, expression was significantly different between GS6 and all other groups except GS7 (3 + 4). We next assessed the diagnostic ability of *PCAT14* to identify prostate cancers versus normal. In both the TCGA and Taylor prostate cancer cohorts, *PCAT14* expression was able to significantly distinguish cancer from normal with an AUC of 0.837 and 0.823 respectively (Figure 3*C*) supporting its utility as a diagnostic biomarker.

Using an alternate approach to further characterize the clinical associations of *PCAT14*, we performed a "guilt-by-association" analysis, assessing the clinical significance of the protein-coding genes most correlated with *PCAT14* (Supplementary Table 2) in the TCGA prostate cancer cohort, leveraging cancer microarray data from the Oncomine resource [21]. As expected, genes positively correlated with *PCAT14* were upregulated in cancer vs normal analysis and were downregulated in clinically advanced prostate cancer (Figure 3*D*). Interestingly, we found a striking association of *PCAT14* correlated genes with concepts related to better prognosis (Figure 3*D*), and these genes were under-expressed in recurrent and hormone refractory prostate cancer suggesting that *PCAT14* may be a marker of better clinical outcomes in prostate cancer. In contrast, genes that positively correlated with *SChLAP1*, a lncRNA known to be associated with clinically aggressive prostate cancer, were found to be overexpressed in advanced prostate cancer as well as in cancer with poor outcomes [15,17].

To further investigate the association of *PCAT14* with favorable clinical outcomes in prostate cancer, we performed Cox regression analysis on a cohort of 355 patients (John Hopkins University (JHU) cohort) who did not receive treatment prior to metastasis (median follow-up 9 years). Univariate analysis showed that, patients with high *PCAT14* expression were significantly associated with better BPFS (P = .000062; HR = 0.59 [0.45–0.76]), MFS (P = .00016; HR = 0.46 [0.32–0.66]), PSS (P = .0067; HR = 0.47[0.27–0.82]) and OS (P = .022; HR = 0.57 [0.35–0.93]) (Figure 4*A-D*). In a Cox multivariate analysis including clinicopathologic variables, *PCAT14* stands out as a significant independent predictor of PSS (P = .0385; HR = 0.55 [0.31–0.97]), MFS (P = .000609; HR = 0.52[0.36–0.76])

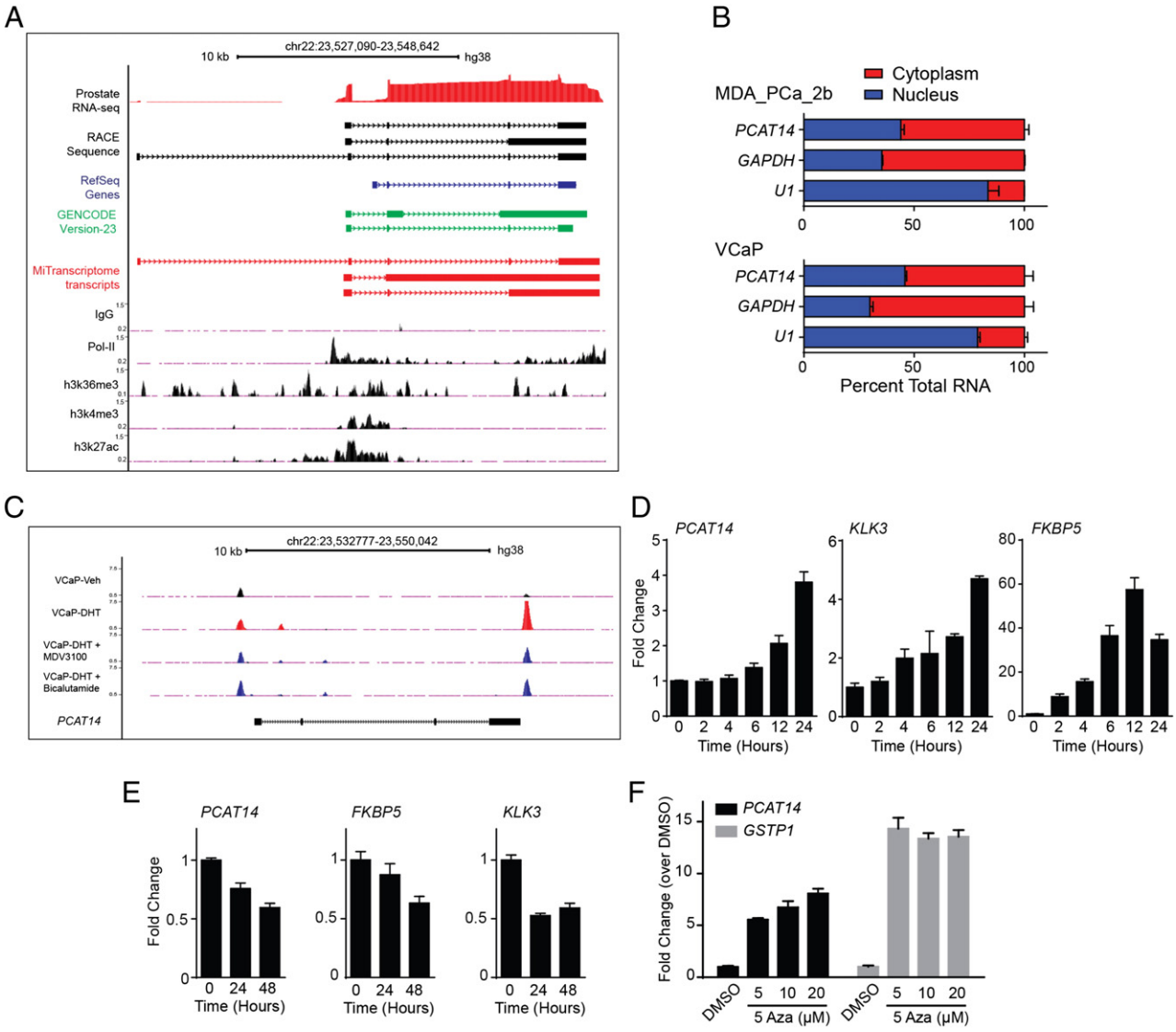

Figure 2. Subcellular localization and regulation of *PCAT14*. A. Genome browser view of *PCAT14* locus. ChIP-seq tracks for H3K4me3, H3K27ac, H3K36me3 and Pol-II generated in prostate cancer VCaP cells are shown. Prostate RNA-seq reads, transcript schematic based on RACE results and Refseq, GENCODE, MiTranscriptome assembly annotations are also provided. Solid blocks indicate exons while thin lines intron and arrows indicate the genomic orientation. B. Bar plots represent the subcellular localization of *PCAT14* in prostate cell lines. *PCAT14* transcript was equally found in both cytoplasmic (red) and nuclear (blue) compartments in both MDA-PCa-2b and VCaP cell lines. GAPDH and U1 RNA were used as controls. C. Genome browser view of the *PCAT14* genomic locus for AR ChIP-seq data tracks obtained from VCaP cells treated with either vehicle (black) or dihydrotestosterone (DHT) alone (Red) or combinations (dark blue) including DHT + MDV3100 and DHT + Bicalutamide. Significant AR binding observed in each data track are represented as peaks. D-E. Histograms represent the expression of *PCAT14*, *TMPRSS2* and *KLK3* in VCaP cells after treatment with 10 nM DHT or with MDV3100 for indicated time points. F. Bar plots represent re-expression of *PCAT14* and *GSTP1* in LNCaP cells after treatment with 5-Aza deoxycytidine (5-Aza) for 5 days at indicated concentrations.

and BRFS (P = .00126, HR = 0.64 [0.49–0.84]), with borderline significance for OS (Table 1, Supplementary Table 3). In addition, we also analyzed the association of *PCAT14* expression with clinical outcome in two independent data sets of 140 (Taylor et al) and 377 (TCGA) patients using the statistical approaches mentioned above [25]. Similar to JHU cohort, high *PCAT14* expression predicted for better BRFS (Figure 4*E*) and MFS (Figure 4*F*). We also show that high PCAT14 expression was predictor of better prognosis in lower Gleason grade samples (Supplementary Figure 3B).

PCAT14 Expression In-Situ

LncRNA detection in cancer tissue sections by RNA in-situ hybridization (RNA-ISH) technology has similar clinical utility as immunohistochemical evaluation of protein biomarkers [16,26]. Hence we evaluated *PCAT14* transcript levels in PCa FFPE tissues using specific probes to perform a RNA-ISH. We first probed a panel of FFPE sections derived from either murine prostate, kidney, lung (negative controls) or xenografts from MDA-PCa-2b cells, a cell line that expresses *PCAT14* at high levels (positive control). As expected,

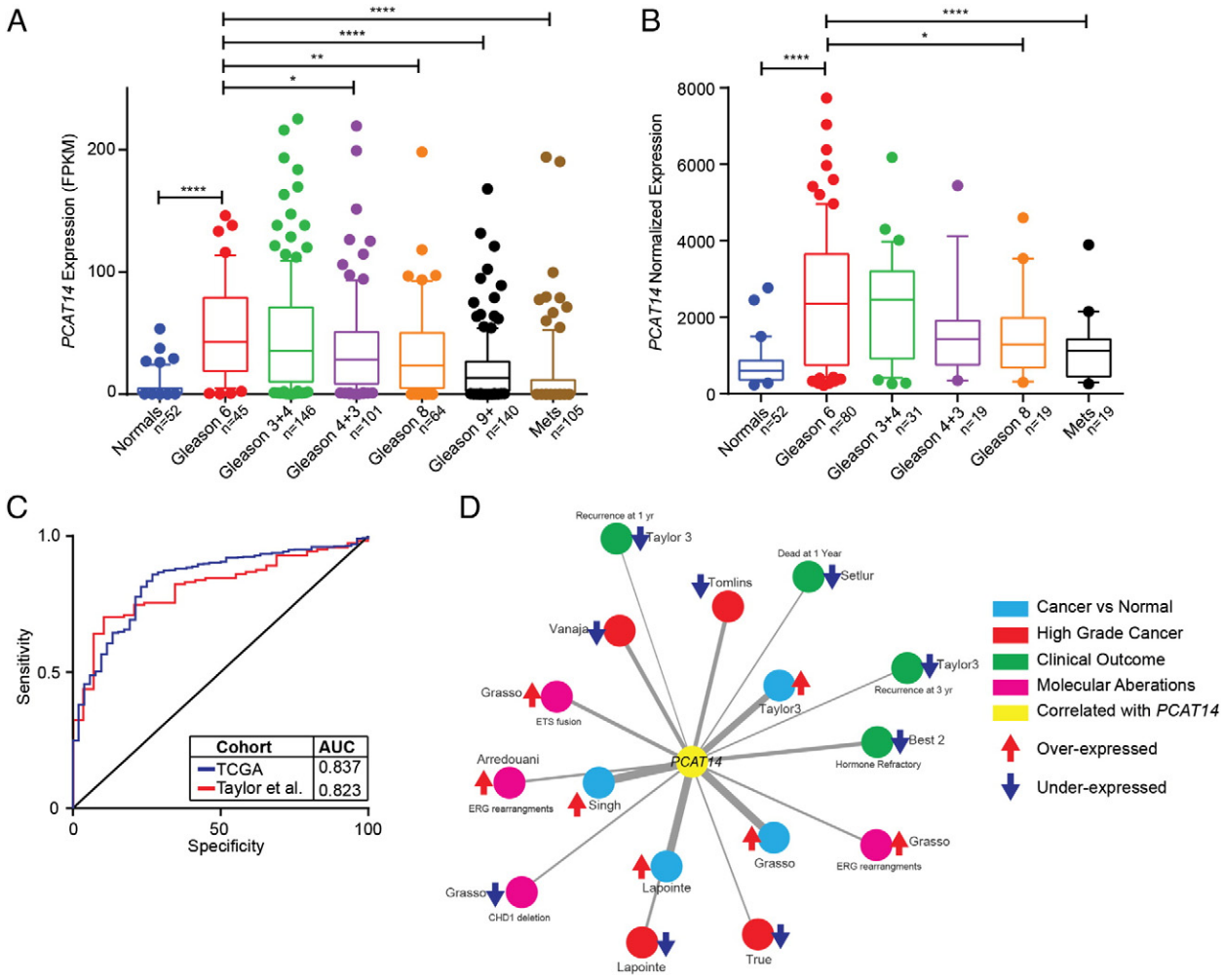

Figure 3. *PCAT14* is marker of low grade tumros. **A-B**. Expression of *PCAT14* in samples distinguished by Gleason grade in TCGA (A), Taylor (B) cohorts. (* = $P < .05$, ** = $P < .01$, **** = $P < .0001$; compared to Gleason 6). C. ROC analysis of *PCAT14* expression in the TCGA and Taylor cohorts. D. Network representation of genes positively correlated with *PCAT14* in localized prostate cancers using Oncomine concepts analysis and visualized with the Force-Directed Layout algorithm in the Cytoscape tool [29]. Node names are assigned according to the author of the primary study [25,30–38]. Nodes are colored according to the concept categories indicated in the figure legend. Thickness of the edges implies higher odds ratio.

high levels of specific signal was present in MDA-PCa-2b xenografts while no expression/staining was seen in the negative control murine tissues (Supplementary Figure 5A and B). Consistent with the cell fractionation data, expression of *PCAT14* was seen in both nuclear and cytoplasmic compartments. Next we obtained frozen and matched formalin fixed paraffin embedded (FFPE) tissues sections derived from a patient radical prostatectomy specimen with Gleason score 3 + 3 = 6 disease. q-PCR analysis on cDNA from frozen tissues derived from this specimen shows a 7–8 fold increase in *PCAT14* expression in cancer compared to the adjacent benign tissue (Figure 5*A*). RNA-ISH also demonstrated that *PCAT14* is differentially expressed in PCa as we saw striking difference of transcript expression with high signals located in the prostatic adenocarcinoma glands and with no/minimum staining in the benign section (Figure 5*B*). To further expand these results, we performed RNA-ISH on a PCa tissue microarray (TMA, n = 129) (Figure 5*C*) and found that *PCAT14* expression was able to distinguish tumor from normal (AUC 0.863) (Figure 5*D*) and was high in Gleason-6 with minimal expression noted in benign tissue or Gleason 8 disease (Figure 5*E*).

Functional Evaluation of PCAT14

Since expression of *PCAT14* was lower in high grade prostate cancer and its expression predicted better outcomes, we hypothesize that *PCAT14* may have tumor suppressive effects. To test this hypothesis, we performed overexpression studies in PC3 and LNCaP cells, prostate cancer cell lines that do not express *PCAT14* (Supplementary Figure 2B, C). To overexpress *PCAT14*, we used a CRISPR (clustered regularly interspaced short palindromic repeat)-Cas9 Synergistic Activation Mediator (SAM) complex [18]. This method allows endogenous overexpression of a gene by recruiting artificial transcriptional factors to the promoter using single-guide RNA (sgRNA-MS2) (See method section for details). We designed 6 sgRNAs targeting the *PCAT14* promoter and tested their ability to induce *PCAT14* expression using HEK293 cells stably expressing transcription factors. We found three sgRNAs that significantly increased *PCAT14* expression in HEK293 cells (Supplementary Figure 5A). We next used these sgRNA to construct PC3 and LNCaP cells stable expressing *PCAT14* (Figure 6*A*). Using two independent sgRNAs we were able to achieve 500 to 1000-fold endogenous overexpression of

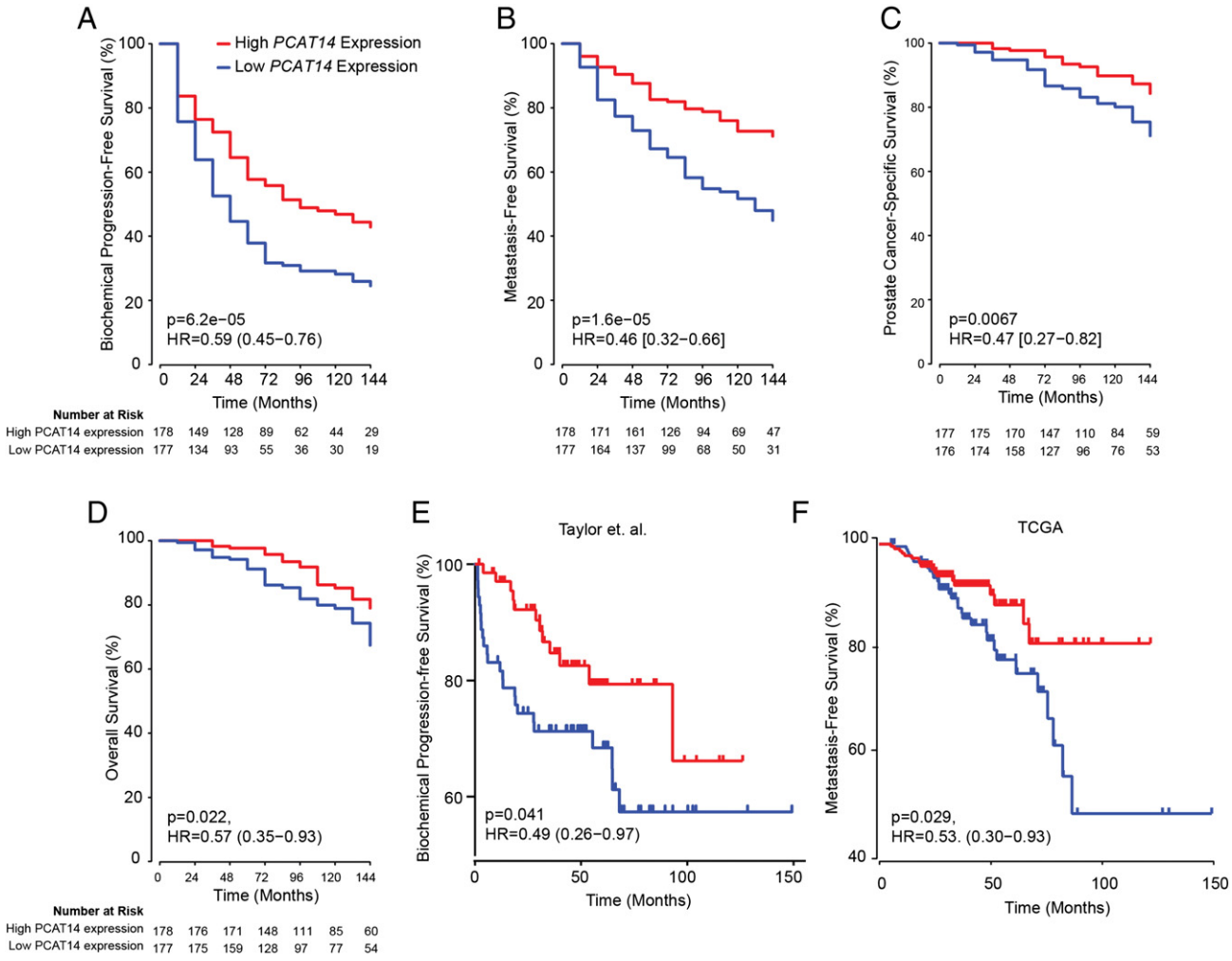

Figure 4. *PCAT14* is a prognostic biomarker. A-D. Kaplan–Meier analyses of prostate cancer outcomes in the John Hopkins cohort. *PCAT14* expression was measured using Affymetrix exon arrays, and subjects were stratified according to their *PCAT14* expression level. Subject outcomes were analyzed for biochemical progression (D) and Metastasis free survival (E), Prostate cancer-specific survival (F) and overall survival (G). Subject outcomes were analyzed for Kaplan–Meier curves, *P* values determined using a log-rank test. E-F. Kaplan–Meier analyses of biochemical progression free survival in the Taylor (E) and Metastasis Free survival in the TCGA (F) cohorts of prostate cancer. Patients were divided into two groups based on the expression level of *PCAT14*. *P* values for Kaplan–Meier curves were determined using a log-rank test.

PCAT14 in PC3 cells (Figure 6*B*) and 20–100 fold overexpression in LNCaP cells (Supplementary Figure 5*B*). While we observed no significant effect of *PCAT14* overexpression on proliferation of PC3 or LNCaP cells (Figure 6*C* and Supplementary Figure 5*C*), overexpression of *PCAT14* lead to suppression of invasion capacity of both PC3 and LNCaP cells (Figure 6*C*, *D*; Supplementary Figure 5*E*, *F*), in line with its prior identified association with clinically indolent disease. We then looked at the effects of *PCAT14* knockdown on cell expressing

Table 1. Multivariate Analysis in JHU Cohort

	Biochemical Recurrence Free Survival		Metastasis Free Survival		Prostate Cancer Free Survival		Overall Survival	
	P-Value	HR [95% CI]	*P*-Value	HR [95% CI]	*P*-Value	HR [95% CI]	*P*-Value	HR [95% CI]
PCAT14 High vs. Low	.00126	0.64 [0.49–0.84]	.000609	0.52 [0.36–0.76]	.0385	0.55 [0.31–0.97]	.0567	0.62 [0.38–1.01]
Age	.818	1 [0.98–1.02]	.65	0.99 [0.96–1.02]	.338	0.98 [0.93–1.02]	.151	0.97 [0.93–1.01]
PSA Int vs. Low	.241	0.83 [0.62–1.13]	.353	0.83 [0.55–1.24]	.385	0.75 [0.4–1.42]	.366	0.77 [0.44–1.35]
PSA High vs. Low	.916	0.98 [0.63–1.52]	.574	0.84 [0.47–1.52]	.463	0.73 [0.31–1.7]	.582	0.81 [0.39–1.7]
Gleason High vs. Low	2.98E-05	1.83 [1.38–2.43]	1.00E-08	3.08 [2.1–4.52]	.000224	3.1 [1.7–5.65]	.000988	2.38 [1.42–3.99]
Seminal vesicle invasion	.0042	1.52 [1.14–2.03]	.453	1.16 [0.79–1.69]	.774	0.92 [0.51–1.66]	.82	0.94 [0.56–1.59]
Surgical margin status	.000533	1.78 [1.28–2.47]	.000276	2.15 [1.42–3.25]	.0487	1.93 [1–3.7]	.0825	1.67 [0.94–2.99]
Extracapsular extension	.456	1.14 [0.81–1.58]	.459	1.21 [0.73–2.03]	.636	0.83 [0.39–1.77]	.816	0.93 [0.48–1.77]
Lymph node invasion	8.98E-12	3.23 [2.31–4.52]	.000164	2.21 [1.46–3.35]	.0616	1.86 [0.97–3.57]	.254	1.42 [0.78–2.6]

HR: Hazard Ratio

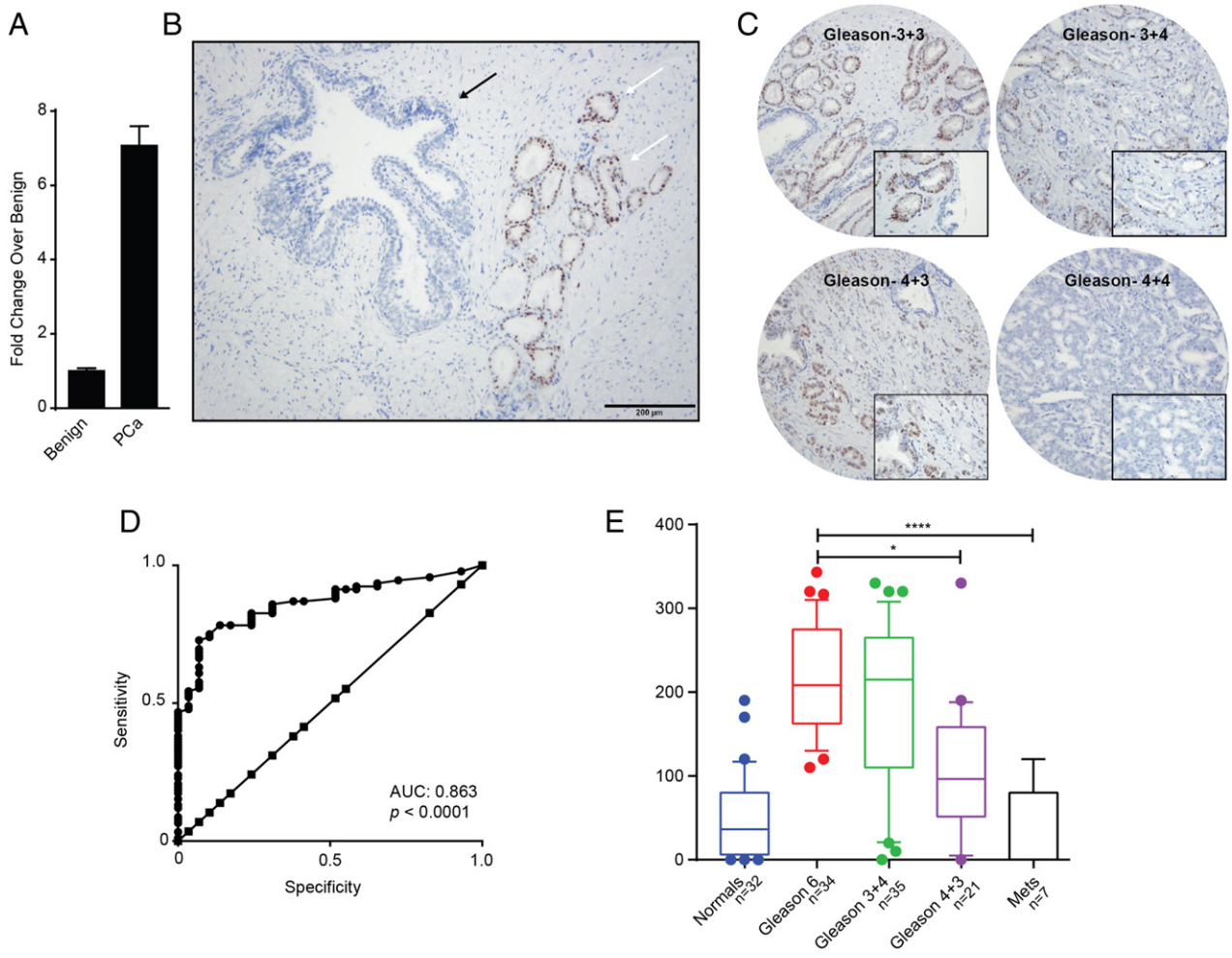

Figure 5. *PCAT14* RNA-ISH in prostate cancer tissues. A. Barplot to show the expression of *PCAT14* in tumor tissue and adjacent benign by qRT-PCR. B. A representative *PCAT14* RNA in-situ hybridization image. White arrows indicate Gleason score 6 disease and black arrows indicate benign glands. C. Representative *PCAT14* In situ hybridization images of human prostate cancer samples of different Gleason grades. D. ROC analysis of *PCAT14* expression in the prostate TMAs. E. Representation of mean *PCAT14* ISH product score for benign prostatic glands (benign), Gleason score 6, Gleason score 3 + 4 = 7, Gleason score 4 + 3 = 7 and Gleason score 8+ clinically localized prostate cancer in a TMA cohort. (** = $P < .01$; compared to benign).

PCAT14 at high levels (VCaP and MDA-PCa-2B). In both MDA-PCa-2b and VCaP cells using 2 independent siRNA as well as 8 independent ASOs we were able to achieve more than 80% knockdown efficiency (Supplementary Figure 5G-J). However, we did not observe a consistent effect on cell proliferation as well as cell invasion (Supplementary Figure 5K-N and data not shown).

Discussion

In this study, we perform a large-scale RNA-sequencing-based analysis of biomarkers associated with indolent versus aggressive prostate cancer and identify the long noncoding RNA *PCAT14* as a marker of low grade and indolent disease. We define the exon structure of *PCAT14* and demonstrate that *PCAT14* is an AR-regulated lncRNA. Using two independent data sets, we show that *PCAT14* is highly upregulated in prostate cancer compared to benign tissue and is able to distinguish prostate cancer from normal tissue with high sensitivity and specificity, suggesting that *PCAT14* can be an excellent diagnostic biomarker. Moreover, we demonstrate that expression of *PCAT14* is prognostic of outcome and is associated with better biochemical progression-free survival, metastases-free survival, and prostate cancer-specific survival. Importantly, we find that *PCAT14* expression is a prognostic biomarker which adds to standard clinicopathologic variables.

As such, *PCAT14* represents a unique biomarker. Most diagnostic biomarkers, such as *PCA3*, can distinguish cancer from normal tissue, but are not prognostic [4]. Conversely, many prognostic biomarkers, such as Ki-67, hold little diagnostic value. It is unclear why *PCAT14* increases significantly in expression during the initial formation of cancer, but then subsequently decreases in expression in disease aggressiveness; this observation requires follow up with further mechanistic studies but is also a feature that gives *PCAT14* value as a biomarker across multiple clinical contexts. Of note, *PCAT14* was also found to be expressed in testicular cancer samples along with prostate cancer, suggesting the role of *PCAT14* in the testicular cancer pathogenesis. However, due to lack of normal testis samples in the TCGA database, it is unclear, at this point, whether *PCAT14* is differentially regulated in testicular cancer compared to normal testis. Recently, the Genotype-Tissue Expression (GTEx) program has

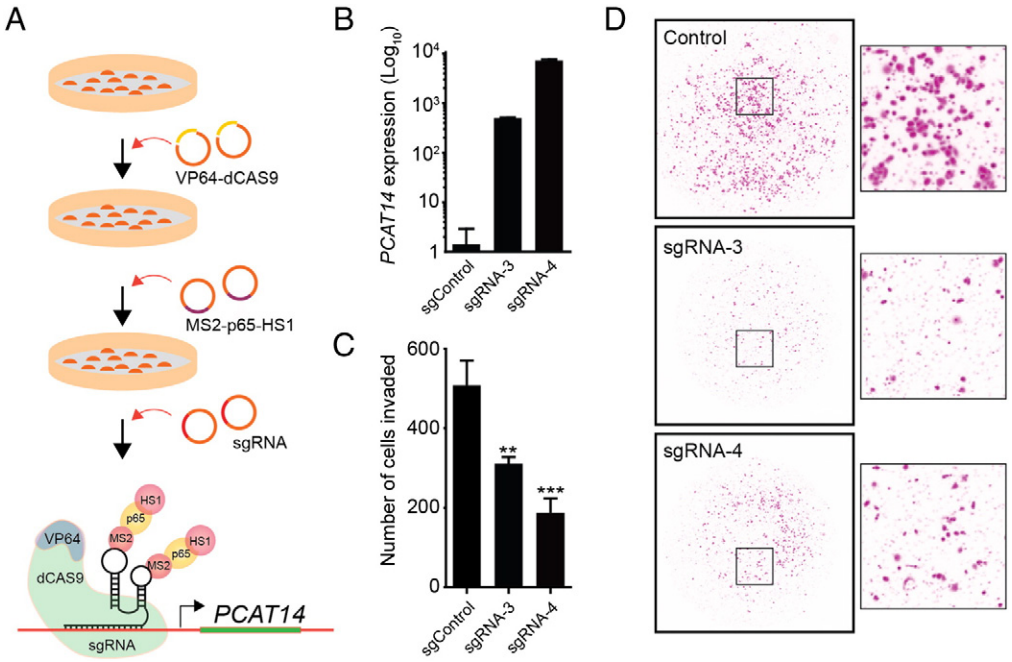

Figure 6. Functional analysis is *PCAT14*. A. Schematic representation of the workflow to endogenously overexpress *PCAT14* in prostate cancer cells using CRISPR/SAM system. B. Bar plots represent fold increase in *PCAT14* level in PC3 cells expressing dCas9–VP64 and MS2–p65–HSF1 with control or 2 independent *PCAT14* sgRNAs. C. Bar plot represent quantification of invaded PC3 cells with or without *PCAT14* expression. D. Representative images of invaded PC3 cells with or without *PCAT14* expression.

generated a large amount of high throughput sequencing data on normal tissue including testis [27]. This data would be useful to look at the role of PCAT14 in testicular carcinoma.

In an attempt to develop a clinical grade assay to detect expression of *PCAT14*, we developed a novel assay, using ISH probes, which can be applied to formalin fixed paraffin-embedded tissues. This ISH assay provides an opportunity to validate our findings in larger cohorts with associated clinical data in the future. Ultimately, an optimized approach for predicting indolent versus aggressive disease will include both clinicopathologic parameters integrated with molecular biomarkers. It is likely that this molecular assay will involve multiplexing multiple biomarkers, and may require combining both tissue-based and urine-based biomarkers. Potential intriguing subsequent studies include the assessment of *PCAT14* and other candidate lncRNAs, in addition to *PCA3*, as urine biomarkers.

There are a several limitations to our study. While we demonstrate the potential value of *PCAT14* expression as a biomarker, it is unclear how *PCAT14* is modulating oncogenic phenotypes, from a mechanistic perspective. Additionally, while we demonstrate the relative specificity of *PCAT14* for both prostate and testicular cancers, the molecular basis underlying this specificity remains to be elucidated. It is known that AR can regulate expression of genes in both prostatic and testicular tissues, but we do not know whether the relative cancer-specificity can be attributed to AR. Clearly, these are important areas for future study.

Overall, our study highlights the need to look at both conventional protein-coding genes and noncoding genes in the search for optimal biomarkers. To our knowledge, there are approximately 20,000 protein coding genes [28], which comprise 2% of the genome. Given our recent study demonstrating that there are close to 60,000 long noncoding RNAs (lncRNAs) [7], many of which are specific to certain cancers, it is clear that these lncRNAs present a relatively underexplored frontier for biomarker development, and that *PCAT14* may represent an initial candidate to be further explored along this frontier.

Conclusion

By performing differential expression analysis between prostate cancer with low vs high Gleason scores, we identified lncRNA *PCAT14* as a prostate cancer- and lineage- specific biomarker of indolent disease. We show that *PCAT14* is an AR-regulated transcript and its overexpression suppresses invasion of prostate cancer cells. Moreover, in multiple independent datasets, *PCAT14* expression associates with favorable outcomes in prostate cancer and adds prognostic value to standard clinicopathologic variables.

Supplementary data to this article can be found online at http://dx.doi.org/10.1016/j.neo.2016.07.001.

Acknowledgments

We thank Sethuramasundaram Pitchiaya, Xia Jiang, Fengyun Su and Ingrid Apel for technical assistance; K. Giles for critically looking over the manuscript and the submission of documents; the University of Michigan Viral Vector Core for generating the lentiviral constructs.

References

[1] Thompson IM, Pauler DK, Goodman PJ, Tangen CM, Lucia MS, Parnes HL, Minasian LM, Ford LG, Lippman SM, and Crawford ED, et al (2004). Prevalence of prostate cancer among men with a prostate-specific antigen level < or =4.0 ng per milliliter. *N Engl J Med* **350**, 2239–2246.

[2] Andriole GL, Crawford ED, Grubb 3rd RL, Buys SS, Chia D, Church TR, Fouad MN, Gelmann EP, Kvale PA, and Reding DJ, et al (2009). Mortality

results from a randomized prostate-cancer screening trial. *N Engl J Med* **360**, 1310–1319.

[3] Schroder FH, Hugosson J, Roobol MJ, Tammela TL, Ciatto S, Nelen V, Kwiatkowski M, Lujan M, Lilja H, and Zappa M, et al (2009). Screening and prostate-cancer mortality in a randomized European study. *N Engl J Med* **360**, 1320–1328.

[4] Leyten GH, Hessels D, Jannink SA, Smit FP, de Jong H, Cornel EB, de Reijke TM, Vergunst H, Kil P, and Knipscheer BC, et al (2014). Prospective multicentre evaluation of PCA3 and TMPRSS2-ERG gene fusions as diagnostic and prognostic urinary biomarkers for prostate cancer. *Eur Urol* **65**, 534–542.

[5] Tomlins SA, Aubin SM, Siddiqui J, Lonigro RJ, Sefton-Miller L, Miick S, Williamsen S, Hodge P, Meinke J, and Blase A, et al (2011). Urine TMPRSS2: ERG fusion transcript stratifies prostate cancer risk in men with elevated serum PSA. *Sci Transl Med* **3**, 94ra72.

[6] Mohler JL, Armstrong AJ, Bahnson RR, D'Amico AV, Davis BJ, Eastham JA, Enke CA, Farrington TA, Higano CS, and Horwitz EM, et al (2016). Prostate Cancer, Version 1.2016. *J Natl Compr Canc Netw* **14**, 19–30.

[7] Iyer MK, Niknafs YS, Malik R, Singhal U, Sahu A, Hosono Y, Barrette TR, Prensner JR, Evans JR, and Zhao S, et al (2015). The landscape of long noncoding RNAs in the human transcriptome. *Nat Genet* **47**, 199–208.

[8] Prensner JR, Iyer MK, Balbin OA, Dhanasekaran SM, Cao Q, Brenner JC, Laxman B, Asangani IA, Grasso CS, and Kominsky HD, et al (2011). Transcriptome sequencing across a prostate cancer cohort identifies PCAT-1, an unannotated lincRNA implicated in disease progression. *Nat Biotechnol* **29**, 742–749.

[9] Sahu A, Singhal U, and Chinnaiyan AM (2015). Long noncoding RNAs in cancer: from function to translation. *Trends Cancer* **1**, 93–109.

[10] Cancer Genome Atlas Research Network. Electronic address scmo, Cancer Genome Atlas Research N (2015). The Molecular Taxonomy of Primary Prostate Cancer. *Cell* **163**, 1011–1025.

[11] Robinson D, Van Allen EM, Wu YM, Schultz N, Lonigro RJ, Mosquera JM, Montgomery B, Taplin ME, Pritchard CC, and Attard G, et al (2015). Integrative clinical genomics of advanced prostate cancer. *Cell* **161**, 1215–1228.

[12] Dobin A, Davis CA, Schlesinger F, Drenkow J, Zaleski C, Jha S, Batut P, Chaisson M, and Gingeras TR (2013). STAR: ultrafast universal RNA-seq aligner. *Bioinformatics* **29**, 15–21.

[13] Liao Y, Smyth GK, and Shi W (2014). featureCounts: an efficient general purpose program for assigning sequence reads to genomic features. *Bioinformatics* **30**, 923–930.

[14] Subramanian A, Tamayo P, Mootha VK, Mukherjee S, Ebert BL, Gillette MA, Paulovich A, Pomeroy SL, Golub TR, and Lander ES, et al (2005). Gene set enrichment analysis: a knowledge-based approach for interpreting genome-wide expression profiles. *Proc Natl Acad Sci U S A* **102**, 15545–15550.

[15] Prensner JR, Zhao S, Erho N, Schipper M, Iyer MK, Dhanasekaran SM, Magi-Galluzzi C, Mehra R, Sahu A, and Siddiqui J, et al (2014). RNA biomarkers associated with metastatic progression in prostate cancer: a multi-institutional high-throughput analysis of SChLAP1. *Lancet Oncol* **15**, 1469–1480.

[16] Mehra R, Shi Y, Udager AM, Prensner JR, Sahu A, Iyer MK, Siddiqui J, Cao X, Wei J, and Jiang H, et al (2014). A novel RNA in situ hybridization assay for the long noncoding RNA SChLAP1 predicts poor clinical outcome after radical prostatectomy in clinically localized prostate cancer. *Neoplasia* **16**, 1121–1127.

[17] Prensner JR, Iyer MK, Sahu A, Asangani IA, Cao Q, Patel L, Vergara IA, Davicioni E, Erho N, and Ghadessi M, et al (2013). The long noncoding RNA SChLAP1 promotes aggressive prostate cancer and antagonizes the SWI/SNF complex. *Nat Genet* **45**, 1392–1398.

[18] Konermann S, Brigham MD, Trevino AE, Joung J, Abudayyeh OO, Barcena C, Hsu PD, Habib N, Gootenberg JS, and Nishimasu H, et al (2015). Genome-scale transcriptional activation by an engineered CRISPR-Cas9 complex. *Nature* **517**, 583–588.

[19] Partridge J and Flaherty P (2009). An in vitro FluoroBlok tumor invasion assay; 2009. J Vis Exp.

[20] Schneider CA, Rasband WS, and Eliceiri KW (2012). NIH Image to ImageJ: 25 years of image analysis. *Nat Methods* **9**, 671–675.

[21] Rhodes DR, Yu J, Shanker K, Deshpande N, Varambally R, Ghosh D, Barrette T, Pandey A, and Chinnaiyan AM (2004). ONCOMINE: a cancer microarray database and integrated data-mining platform. *Neoplasia* **6**, 1–6.

[22] Aytes A, Mitrofanova A, Lefebvre C, Alvarez MJ, Castillo-Martin M, Zheng T, Eastham JA, Gopalan A, Pienta KJ, and Shen MM, et al (2014). Cross-species regulatory network analysis identifies a synergistic interaction between FOXM1 and CENPF that drives prostate cancer malignancy. *Cancer Cell* **25**, 638–651.

[23] Varambally S, Dhanasekaran SM, Zhou M, Barrette TR, Kumar-Sinha C, Sanda MG, Ghosh D, Pienta KJ, Sewalt RG, and Otte AP, et al (2002). The polycomb group protein EZH2 is involved in progression of prostate cancer. *Nature* **419**, 624–629.

[24] Asangani IA, Dommeti VL, Wang X, Malik R, Cieslik M, Yang R, Escara-Wilke J, Wilder-Romans K, Dhanireddy S, and Engelke C, et al (2014). Therapeutic targeting of BET bromodomain proteins in castration-resistant prostate cancer. *Nature* **510**, 278–282.

[25] Taylor BS, Schultz N, Hieronymus H, Gopalan A, Xiao Y, Carver BS, Arora VK, Kaushik P, Cerami E, and Reva B, et al (2010). Integrative genomic profiling of human prostate cancer. *Cancer Cell* **18**, 11–22.

[26] Mehra R, Udager AM, Ahearn TU, Cao X, Feng FY, Loda M, Petimar JS, Kantoff P, Mucci LA, and Chinnaiyan AM (2015). Overexpression of the Long Non-coding RNA SChLAP1 Independently Predicts Lethal Prostate Cancer. *Eur Urol.* pii: S0302-2838(15)01211-7. doi: 10.1016/j.eururo.2015.12.003. [Epub ahead of print].

[27] Consortium GT (2015). Human genomics. The Genotype-Tissue Expression (GTEx) pilot analysis: multitissue gene regulation in humans. *Science* **348**, 648–660.

[28] Consortium EPBirney E, Stamatoyannopoulos JA, Dutta A, Guigo R, Gingeras TR, Margulies EH, Weng Z, Snyder M, and Dermitzakis ET, et al (2007). Identification and analysis of functional elements in 1% of the human genome by the ENCODE pilot project. *Nature* **447**, 799–816.

[29] Shannon P, Markiel A, Ozier O, Baliga NS, Wang JT, Ramage D, Amin N, Schwikowski B, and Ideker T (2003). Cytoscape: a software environment for integrated models of biomolecular interaction networks. *Genome Res* **13**, 2498–2504.

[30] Grasso CS, Wu YM, Robinson DR, Cao X, Dhanasekaran SM, Khan AP, Quist MJ, Jing X, Lonigro RJ, and Brenner JC, et al (2012). The mutational landscape of lethal castration-resistant prostate cancer. *Nature* **487**, 239–243.

[31] Lapointe J, Li C, Higgins JP, van de Rijn M, Bair E, Montgomery K, Ferrari M, Egevad L, Rayford W, and Bergerheim U, et al (2004). Gene expression profiling identifies clinically relevant subtypes of prostate cancer. *Proc Natl Acad Sci U S A* **101**, 811–816.

[32] Vanaja DK, Cheville JC, Iturria SJ, and Young CY (2003). Transcriptional silencing of zinc finger protein 185 identified by expression profiling is associated with prostate cancer progression. *Cancer Res* **63**, 3877–3882.

[33] Arredouani MS, Lu B, Bhasin M, Eljanne M, Yue W, Mosquera JM, Bubley GJ, Li V, Rubin MA, and Libermann TA, et al (2009). Identification of the transcription factor single-minded homologue 2 as a potential biomarker and immunotherapy target in prostate cancer. *Clin Cancer Res* **15**, 5794–5802.

[34] Best CJ, Gillespie JW, Yi Y, Chandramouli GV, Perlmutter MA, Gathright Y, Erickson HS, Georgevich L, Tangrea MA, and Duray PH, et al (2005). Molecular alterations in primary prostate cancer after androgen ablation therapy. *Clin Cancer Res* **11**, 6823–6834.

[35] Singh D, Febbo PG, Ross K, Jackson DG, Manola J, Ladd C, Tamayo P, Renshaw AA, D'Amico AV, and Richie JP, et al (2002). Gene expression correlates of clinical prostate cancer behavior. *Cancer Cell* **1**, 203–209.

[36] True L, Coleman I, Hawley S, Huang CY, Gifford D, Coleman R, Beer TM, Gelmann E, Datta M, and Mostaghel E, et al (2006). A molecular correlate to the Gleason grading system for prostate adenocarcinoma. *Proc Natl Acad Sci U S A* **103**, 10991–10996.

[37] Setlur SR, Mertz KD, Hoshida Y, Demichelis F, Lupien M, Perner S, Sboner A, Pawitan Y, Andren O, and Johnson LA, et al (2008). Estrogen-dependent signaling in a molecularly distinct subclass of aggressive prostate cancer. *J Natl Cancer Inst* **100**, 815–825.

[38] Tomlins SA, Mehra R, Rhodes DR, Cao X, Wang L, Dhanasekaran SM, Kalyana-Sundaram S, Wei JT, Rubin MA, and Pienta KJ, et al (2007). Integrative molecular concept modeling of prostate cancer progression. *Nat Genet* **39**, 41–51.